

A new method for assessment of changes in retinal blood flow

Eric T. Lee, Paul G. Rehkopf, Joseph W. Warnicki, Thomas Friberg, David N. Finegold and Edward G. Cape

University of Pittsburgh, Schools of Medicine and Engineering, Pittsburgh, Pennsylvania, USA

Received 8 April 1996, accepted 16 August 1996

ABSTRACT

This study validates the use of residence time distribution (RTD) functions in human subjects to assess changes in retinal flow by using the widely recognized model of flow changes due to oxygen breathing. Changes in retinal blood flow may provide important information for clinical decision-making in several populations, including those with diabetic retinopathy, sickle cell disease and retinitis pigmentosa. Normal volunteer subjects were studied before and after oxygen breathing. After IV injection, relative fluorescence was obtained using scanning laser ophthalmoscopy/image processing in all vessel branches (average, 17). For each experiment, 64 frames (2/s) were digitized and were normalized using the RTD method. Vessel diameters were measured using densitometry techniques on fundus photos, where the diameter data made it possible to weight each vessel according to relative cross-sectional area to obtain a true mean circulation time (MCT). MCT increased for the group of subjects when breathing oxygen compared to normal air ($P=0.001$), representing a decrease in retinal blood flow. Average MCT increased 2.82 ± 2.51 s for all subjects, with an increase of 2.93 ± 2.26 s in repeat trials for one subject. The proposed method uses information from all retinal vessels and allows the assessment of overall, as well as selected, regional retinal flow. It is more comprehensive than previous methods analysing single vessel flow. This method will be potentially useful for assessing hemodynamic changes in the retina associated with a wide range of eye disease. © 1997 Elsevier Science Ltd for IPEM.

Keywords: Retinal blood flow, scanning laser, hemodynamics, fluorescein angiography

Med. Eng. Phys., 1997, Vol. 19, 125–130, March

1. INTRODUCTION

Current methods for evaluating retinal blood flow include the use of fluorescein angiography and laser Doppler velocimetry. However, one common denominator found among these techniques is the use of single vessels after branching (one artery; one vein) to quantify flow. This study addresses the hypothesis that residence time distribution functions can be used to detect global changes in retinal blood flow and can be implemented in humans using scanning laser ophthalmoscopic data. Since the method uses information from all retinal vessels, it is potentially more representative of overall retinal flow than previous methods analysing single vessel flow. This method will have a primary application in patients with diabetic retinopathy, the leading cause of blindness in the United States. Deterioration of vision in this condition is believed to be associated with a breakdown in the autoregulatory

mechanisms that control flow in the retinal vasculature. In this study, retinal flow is intentionally altered in normal subjects to test the applicability of our method in humans.

2. THEORY

Residence time distribution functions are normalized mathematical models reflecting the fraction of injected contrast with a specific age within a defined region of interest^{1–3}. They implicitly include mean circulation times and are independent of the amount of contrast injected. Functions for individual vessels can be combined into composite functions that potentially represent the overall retinal flow.

The residence time distribution function, $F(t)$, represents the integrated fraction of injected contrast that has passed through a window at time t . The value of $1-F(t)$ is the volume fraction that has remained between the point of injection and the window for a time less than t . For an injected bolus of fluorescein, $F(t)$ at a downstream window is, by definition:

$$F(t) = \frac{\int_0^t x_f M dt}{m_T}, \quad (1)$$

where x_f is the mass fraction of fluorescein at the window, M is the mass flow rate, and m_T is the total mass of fluorescein passing through the window². Discretizing Equation (1) and defining it in terms of concentrations of fluorescein, one can obtain Equation (2):

$$F(t) = \frac{\sum_0^t C_f}{\sum_0^\infty C_f}. \quad (2)$$

Using scanning laser ophthalmoscopic and image processing techniques, acquisition of fluorescein concentration at windows placed on the retinal vessels distal to injection (intravenous) is made possible (see Methods). The time it takes for a particle to pass through the system is called its residence time. Residence time distribution functions can be used to obtain a value for mean residence time¹:

$$t_{\text{mean}} = \int_{t=0}^{t=\infty} t \left(\frac{dF(t)}{dt} \right) dt. \quad (3)$$

For the simple case of a single artery-vein pair, the mean residence time is calculated between the injection location and the artery by placing a window on the artery and calculating t_{mean} based on Equation (3). Likewise, a mean residence time is obtained between the injection location and a single vein by placing a window on the vein and calculating a different t_{mean} from Equation (3). By conservation of mass, the artery t_{mean} can be subtracted from the vein t_{mean} to obtain an estimate of the mean circulation time (MCT) between the two windows or, in this case, through the capillary bed (t_{mean} calculated from the vein window must be larger than t_{mean} calculated from the artery; instantaneous passage through the capillary would make them equal).

The actual retinal vasculature, however, consists of multiple arteries feeding into capillary beds with multiple veins returning flow to the heart. Residence time distribution functions from multiple arteries (Figure 1) can be combined by weighting each artery according to its cross-sectional area. The composite arterial and venous curve data are then used to calculate a mean circulation time (MCT) based on all vessels using the following equation:

$$\begin{aligned} \text{MCT} &= t_{\text{mean}}(\text{veins}) - t_{\text{mean}}(\text{arteries}) \quad (4) \\ &= \sum_{n=1}^b \left(\frac{\sum_{t=0}^{t=\infty} A_n \cdot C_{f_n} \cdot t}{\sum_{t=0}^{t=\infty} A_n \cdot C_{f_n}} \right) - \sum_{m=1}^a \left(\frac{\sum_{t=0}^{t=\infty} A_m \cdot C_{f_m} \cdot t}{\sum_{t=0}^{t=\infty} A_m \cdot C_{f_m}} \right), \end{aligned}$$

where t is time, a and b are the number of arteries and veins, respectively, $C_{f/n}$ is the concentration

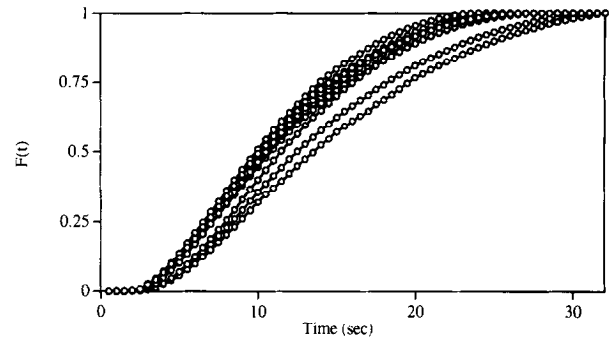


Figure 1 Residence time distribution functions for each individual artery for one subject. Note the variability from artery to artery. A similar figure can be demonstrated for the individual veins

of fluorescein at the window of the n th vein, $C_{f/m}$ is the concentration of fluorescein at the window of the m th artery, and A_m , A_n are dimensionless factors that weight each artery and vein with respect to the total cross-sectional area of all the arteries and veins, respectively. The values of A_m and A_n for a particular artery and vein are calculated by dividing the cross-sectional area of the particular vessel by the total cross-sectional area of all the arteries or veins.

3. MATERIALS AND METHODS

The proposed method was tested in a study of 16 subjects (eight males, eight females; mean age was 25.1; range 21–39). The widely accepted method of air vs oxygen breathing was chosen to produce intentional flow changes in the retina. All test subjects were volunteers and were chosen as normals based on the criteria that they had no history of, or any observable, retinal pathology and none had any disease or physical impairments that affected either the visual or cardiovascular system. The right eye was studied in all subjects. Prior to fluorescein angiography, red-free fundus photographs were taken using a Zeiss Model FF3 Oberkochen fundus camera. Determinations of axial length using ultrasonography, K-reading, and refractive index measurements were also obtained. Fundus photographs were taken at least 30 min prior to the experimental procedure, to eliminate any possible effects of camera flash on blood flow.

Immediately before fluorescein angiography, the subject's blood pressure and heart rate were measured. A transcutaneous oxygen monitor (Transcom 807) was used to measure continuously the oxygen levels during each experiment. Initially, the subject was injected with 1.5 ml of 25% sodium fluorescein (antecubital vein) while breathing air. A Rodenstock SLO 101 scanning laser ophthalmoscope (SLO) was used to obtain a video record of the angiogram. The SLO provides direct scanning of the retina with high directivity, thus allowing improved imaging with reduced light trauma to the eye (Figure 2). The SLO induces dye fluorescence by emitting an argon blue (488-nm-wavelength) beam on to the retinal vasculature, and this fluorescence is recorded for post-angiogram digital image processing.

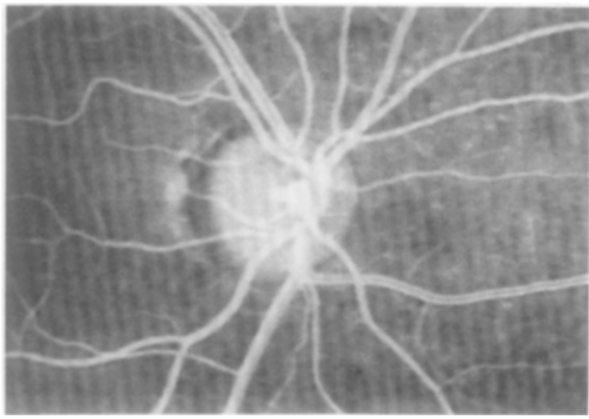


Figure 2 An image from the SLO showing complete contrast fluorescence in the arteries and initial filling of contrast in the veins

After data acquisition for air breathing, the subject was asked to breathe 100% oxygen supplied through a breathing mask at a rate of 4 l/min, during which, a transcutaneous pO_2 was measured using the Transcom 807. After approximately 15–20 min, a steady state transcutaneous pO_2 was achieved, indicating an elevated arterial pO_2 (p_aO_2) oxygen level (all subjects reached steady state and the level varied from subject to subject). The heart rate and blood pressure of the subject were recorded for the new conditions. The fluorescein angiogram and data acquisition processes were then repeated by injecting another 1.5 ml of 25% sodium fluorescein into the antecubital vein. Upon completion of oxygen breathing, 3 ml of fluorescein produces a relatively high background intensity level, making additional measurements impossible. Therefore, a third procedure to determine baseline changes upon returning to air breathing was not performed.

Image processing was then performed on the recorded fluorescein angiogram. Using a Megavision 1024XM Image Processor, the recorded data were digitized and placed on hard disk media at a rate of 2 frames/s for a total of 64 frames. All of the 64 images were aligned to a reference image (one of the 64 images) to compensate for eye movement. Analysis windows were placed approximately one-half of a disc diameter from the edge of the optic disc on vessels of interest in the reference image. Vessels of interest were chosen to comprise a closed loop of arterics and veins that supply blood to, and remove blood from, the retina, thus assuring a conservation of mass. Windows were placed proximal to bifurcations for arteries and distal to bifurcations for veins whenever possible to minimize the total number of windows required (average number of windows=17). The images were then recalled automatically and in sequential order, and the image processor calculated the gray levels corresponding to the fluorescence level in all analysis windows. Fluorescein intensities are considered to be proportional to fluorescein concentrations for the doses of sodium fluorescein injected peripherally.

Fundus photographs taken for each subject as described above were used to measure vessel

diameters as follows. These photographs were digitized at high resolution (1850 pixels/inch) and were displayed using Global Lab. Image, an image processing and analysis program by Data Translation. The software package contains tools that allow gray values along a specified line segment to be measured and stored. Using microdensitometric techniques, vessel diameters were calculated by drawing a pixel width a line perpendicular to the axis of a vessel and obtaining an intensity profile along a line. Additional software was developed to allow 20 adjacent lines to be obtained and averaged to account for background variability. A typical intensity profile is shown in *Figure 3*. The diameter of the vessel (in pixels) is determined by measuring the half-height width of the intensity profile as indicated in *Figure 3*^{1,5}. Note that the dip at the center of the profile represents the reflection of light at the back of the vessel. The diameter obtained is expressed in units of pixels and can be converted to true dimensions in the manner of Littmann⁶, taking into account the refractive power of the eye, corneal curvature and axial length.

The retinal arteriovenous (A–V) mean circulation times (MCT) for each subject were evaluated based on the theory presented above. Before transformation into a residence time distribution function, intensity levels for each analysis window were fitted with an exponential so that any recirculation effects were removed. This is demonstrated for a typical intensity curve in *Figure 4*. Concentration curves were then converted to residence time distribution functions (RTDs), and individual RTDs were combined by weighting each vessel according to its cross-sectional area as described above, resulting in one composite function (CRTD) for arteries, and another for veins. Each of the two CRTDs was used to calculate a MCT (arterial and venous), and the retinal A–V MCT for a trial was calculated by taking the difference between the MCT for the arteries and veins. This retinal A–V MCT was calculated for both air and oxygen breathing for each subject, and a statistical comparison was made using a paired *t*-test.

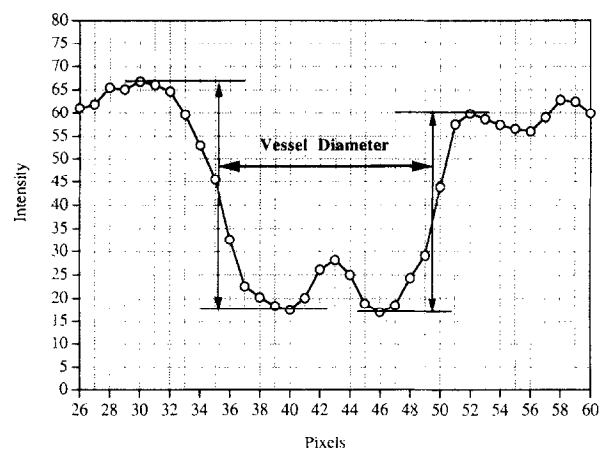


Figure 3 The diameter of the vessel (in pixels) is determined by measuring the half-width of the intensity profile. The dip at the center of the profile represents the reflection of light at the back of the vessel

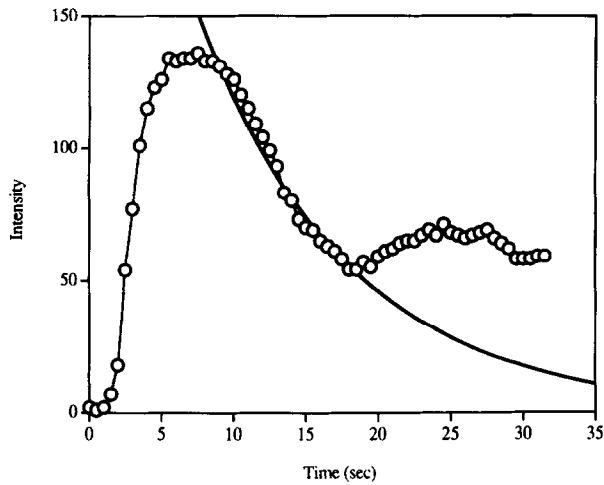


Figure 4 A typical intensity curve for a single analysis window. Intensity levels for each analysis window were fitted with an exponential so that any recirculation effects were removed

4. RESULTS

Table 1 summarizes the number of analysis windows that were placed on arteries and veins, and transcutaneous blood oxygen levels (TC pO₂) before and after O₂ breathing, for each subject. (It has been documented that TC pO₂ levels are approximately 80% of the arterial blood oxygen level⁷.) Two subjects were excluded due to excessive vessel tortuosity (see below). The MCTs for the remaining 14 subjects during air and oxygen breathing are outlined in Table 2. MCT increased for the group of subjects when breathing oxygen compared to normal air ($P=0.001$). MCTs ranged from 1.65 s to 5.54 s for air and 3.35 s to 10.8 s for oxygen breathing. The average increase in MCT was 2.82 ± 2.51 s. Only subject 3629 exhibited a negative change after O₂ breathing (MCTs were 3.68 s for air and 2.09 s for oxygen) possibly due to variable subject state between air and oxygen breathing, despite controlled conditions.

Due to excessive tortuosity and overlapping of vessels in the two excluded subjects, the method of tracking fluorescence at several analysis windows proved to be impossible with the current imaging technology. Figure 5 shows one of these

Table 2 Weighted mean circulation times using vessel diameters

Subject	MCT for airbreathing (s)	MCT for O ₂ breathing (s)	Change (increase)
3622	3.53	5.85	2.32
3624	5.08	10.6	5.52
3629	3.68	2.09	-1.59
3706	2.99	4.85	1.86
3707	3.05	5.87	2.82
3720	3.93	4.46	0.53
3722	1.65	7.99	6.34
4718	3.50	4.44	0.94
4719	2.91	3.35	0.44
4720	2.36	6.05	3.69
4929	5.68	8.72	3.04
4A13	5.18	9.40	4.22
4A18	3.20	10.8	7.60
4A20	5.54	7.24	1.70

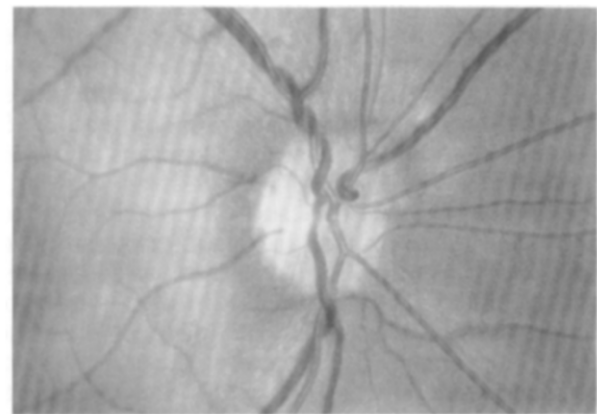


Figure 5 A fundus photograph of one of the excluded subjects. The tortuous, rope-like nature of the vessels in the upper portion of the image prohibited accurate tracking of intensities in this area

images. The vessels are intertwined in a rope-like fashion shown in the upper portion of the image. The eccentricities that justified excluding these points are thus clearly detectable. Interestingly, the two subjects with morphologic eccentricities were siblings.

Repeated trials were performed on one of the subjects, subject 3624. Two additional trials were

Table 1 General subject data

Subject	Age	Number of arteries	Number of veins	TC pO ₂ (mmHg) (air breathing)	TC pO ₂ (mmHg) (O ₂ breathing)
3622	24	6	10	84	210
3624	23	10	7	64	134
3629	24	10	8	69	162
3701	23	10	8	79	295
3706	23	10	8	46	236
3707	39	12	6	88	148
3720	23	9	9	70	122
3722	23	9	7	69	101
3803	21	14	5	71	135
4718	26	10	11	68	186
4719	25	12	8	101	306
4720	24	12	10	65	163
4929	22	11	4	76	90
4A13	25	14	6	73	163
4A18	25	12	5	77	122
4A20	32	9	5	71	131

conducted 124 and 126 days after the initial trial. All procedures were performed in the same fashion as the initial trial. MCT increased by 2.93 ± 2.26 s. comparing O_2 to air breathing. As postulated, the multiple runs for this subject show a consistent decrease in retinal blood flow during hyperoxia.

Total arterial and venous cross-sectional areas measured from the digitized fundus photos are listed in Table 3. The average total arterial area was $(5.18 \pm 1.16) \times 10^4 \mu m^2$ and the average total venous area was $(6.01 \pm 0.65) \times 10^4 \mu m^2$. Fundus coloration did not have any effect on vessel measurements, since a diameter measurement for a particular vessel is based upon the fluorescence gradient from the vessel to the adjacent background tissue.

5. DISCUSSION

This paper describes a method that uses data from a closed set of retinal branches to produce a consistent and representative assessment of flow. The average mean circulation time calculated using this new method was 3.73 ± 1.22 s during normal air breathing. Hickam and Frayser⁸ determined an average MCT of 4.7 ± 1.1 s in 29 normal males during air breathing using their photographic method. These MCTs are slightly higher than those found in this study, but this may be attributed to the fact that they have based their measurements on only one artery-vein pair. *Other studies are consistent with our results.* Bulpitt and Dollery⁹ found a wide scatter of MCTs in seven subjects, with an average in the superior temporal system of 3.41 ± 1.68 s. Using a modified method of that used by Hickam and Frayser, Kohner¹⁰ calculated MCTs in nine normal subjects to be about 3.8 s, virtually identical to that in this study. It is important to keep in mind that methods using single artery-vein pairs most often select a dominant vessel branching from the ophthalmic artery or vein, and the lack of attention to subtle changes occurring in less predominant vessels may contribute to overestimation.

A regulatory response is believed to effectively maintain a constant oxygen supply to the retina to

satisfy metabolic demands. Therefore, during hyperoxia, one should see a reduced flow through the retina implying longer mean circulation times (MCT). This phenomenon was demonstrated clearly in the current study. An *in-vitro* model has also demonstrated the autoregulatory response to changes in pO_2 in the isolated cat eye¹¹. Hyperoxia showed the expected decrease in retinal flow, and hypoxia, or decreased pO_2 levels, showed flow rate increases in this *in-vitro* study. By producing a similar response in normal human subjects, we were able to test our proposed technique, which clearly showed changes consistent with hyperoxia.

This study showed an average increase in MCT during oxygen breathing of 2.82 ± 2.51 s in 14 subjects. Hickam and Frayser⁸ conducted single vessel experiments where subjects also breathed 100% oxygen. They concluded that inhalation of oxygen prolonged MCTs. Grunwald *et al.*¹² studied blood flow changes using bidirectional laser Doppler velocimetry (LDV) and also found increased MCT with oxygen breathing.

Total arterial and venous cross-sectional areas were also measured for each subject in this study. The average total areas for the arteries and veins were $(5.18 \pm 1.16) \times 10^4 \mu m^2$ and $(6.01 \pm 0.65) \times 10^4 \mu m^2$, respectively. The value for the arteries compares well with a study by Feke and others¹³ where they compared total arterial areas for normals and diabetic patients. Their results were $(4.7 \pm 0.7) \times 10^4 \mu m^2$ for normals and $(5.5 \pm 1.0) \times 10^4 \mu m^2$ for diabetics, which is expected since vessel dilation accompanies advancing retinopathy.

5.1. Limitations

The rate of decay calculated by the exponential fit is dependent on the degree of noise encountered during the image processing stage. If the noise is sufficiently high, then this increases the degree of scatter of data points for a particular vessel. The exponential fit and its corresponding rate of decay are then subject to variability. This degree of variability is a by-product of the limitations of the image processing stage, and by refining registration of images, this variable can be effectively minimized.

The proposed method is dependent upon the use of area fractions to weight accurately each vessel according to its respective diameter. Two commonly observable conditions that may introduce errors are that veins constrict more than arteries during hyperoxia, and that smaller vessels constrict proportionately more than larger vessels in response to oxygen and constrictor drugs. Deutsch *et al.*¹⁴ have reported that, during 100% oxygen breathing, the caliber of superotemporal retinal arteries and veins constricted by an average of 9.4% and 15.9%, respectively. Grunwald¹² found that main superior or inferior temporal veins decreased in diameter by $16 \pm 5\%$ in 19 eyes. Riva *et al.*¹⁵ reported an average arterial constriction of 12.1%. Hague *et al.*¹⁶ studied the caliber changes during prolonged hyperoxia and found that the mean artery constriction was $15.3 \pm 4.6\%$.

Table 3 Total cross-sectional areas

Subject	Total arterial area ($10^4 \mu m^2$)	Total venous area ($10^4 \mu m^2$)
3622	4.10	6.22
3624	4.53	6.64
3629	3.74	5.48
3706	4.50	6.45
3707	6.97	5.70
3720	4.39	5.55
3722	6.17	6.86
4718	3.76	7.21
4719	4.72	5.80
4720	4.90	6.04
4929	5.35	5.30
4A13	6.24	5.11
4A18	7.29	5.28
4A20	5.91	6.47

and the mean venous constriction was $21.8 \pm 4.3\%$. Hickam and Frayser⁸ showed an $11.6 \pm 4.7\%$ diameter reduction for arteries and $14.9 \pm 6.5\%$ for the veins during hyperoxia as compared to air breathing. The work done by these investigators shows that vessel constrictions are highly variable, depending upon the individual and the diameter measurement technique. In the current study, area fractions are computed separately for the arteries and veins to minimize any variability resulting from these effects. Hickam and Frayser⁸, as well as Dollery and associates^{17,18}, report that smaller retinal arteries and veins constrict proportionally more than larger vessels in response to oxygen and constrictor drugs. However, the result of small vessels constricting proportionally more than larger ones will only increase the effect of large vessels on MCTs. In other words, the already small contribution to flow provided by small vessels can only decrease if they constrict relatively more than large vessels. Therefore, the overall effect on the calculation of MCT will be minimally affected. *This can be demonstrated by using one of the subjects in this study (subject 3720).* Suppose that, after oxygen breathing, the following occurs: the large arteries constricted by 12%, the small arteries constricted by 24%, the large veins constricted by 16.5%, and the small veins constricted by 33%; then MCT is 4.54 s (15.5% change). From Table 2, which does not account for constriction, after oxygen breathing, the MCT was 4.46 (13.5% change). We see, from this example, that the effect of small vessels constricting more than larger vessels has only a small effect on MCTs. Therefore, the assumption that area fractions remain constant after oxygen breathing is a strong one in the context of the current study.

5.2. Clinical implications

Changes in retinal blood flow may provide important information for clinical decision-making in several populations, including those with diabetic retinopathy, sickle cell disease and retinitis pigmentosa. The method proposed here, which should eliminate much of the variability in previously reported single vessel studies, can be implemented on available and widely used clinical instruments. The Rodenstock SLO is a commercially available instrument, and the image processing programs and equipment are easily obtained. Custom software was written to analyse the data according to the theory presented above.

5.3. Conclusions

In summary, this study has verified the use of residence time distribution functions as a sensitive assessment of changes in retinal blood flow. The results of this study demonstrate that a comprehensive evaluation of global retinal flow may be obtained from multiple vessel studies using the scanning laser ophthalmoscope and image processing techniques. Furthermore, the method is not limited to only a global assessment of retinal flow, since residence time distribution functions

for vessel subsets can be potentially extracted to describe local variations in flow.

ACKNOWLEDGEMENTS

This work was supported in part by the Children's Hospital of Pittsburgh, the Pennsylvania Lions Sight Conservation and the Eye Research Foundation, and the Murray Foundation for Eye Research Inc.

REFERENCES

1. Danckwerts, P. V., Continuous flow systems. *Chemical Engineering Science*, 1953, **2**, 1–13.
2. Hill, C. G., *An Introduction to Chemical Engineering and Reactor Design*. Wiley, New York, 1977, p. 388.
3. Levenspiel, O., *Chemical Reaction Engineering: an Introduction to the Design of Chemical Reactors*. Wiley, New York, 1962, p. 243.
4. Brinckmann-Hansen, O., Heier, H. and Myhre, K., Fundus photography of width and intensity profiles of the blood column and the light reflex in retinal vessels. *Acta Ophthalmologica*, 1986, **179**, 20–28.
5. Delori, F. C., Fitch, K. A., Feke, G. T., Deupree, D. M. and Weiter, J. J., Evaluation of micrometric and microdensitometric methods for measuring the width of retinal vessel images on fundus photographs. *Graef's Archives of Clinical and Experimental Ophthalmology*, 1988, **226**, 393–399.
6. Littmann, H., The determination of the real size of an object on the fundus of the living eye. *Klinische Monatsblätter Fur Augenheilkunde*, 1982, **180**, 286–289.
7. Tremper, K. K. and Shoemaker, W. C., Transcutaneous oxygen monitoring of critically ill adults with and without low flow shock. *Critical Care Medicine*, 1981, **9**, 706–709.
8. Hickam, J. B. and Frayser, R., Studies of the retinal circulation in man. *Circulation*, 1966, **33**, 302–316.
9. Bulpitt, C. J. and Dollery, C. T., Estimation of retinal blood flow by measurement of the mean circulation time. *Cardiovascular Research*, 1971, **5**, 406–412.
10. Kohner, E. M., Retinal blood flow in diabetes. In *Diabetic Retinopathy*, ed. J. R. Lynn, W. B. Snyder and A. Vaiser. Grune and Stratton, New York, 1974, pp. 71–79.
11. Papst, N., Demant, E. and Niemeyer, G., Changes in pO_2 induce retinal autoregulation *in vitro*. *Graef's Archives of Clinical and Experimental Ophthalmology*, 1982, **219**, 6–10.
12. Grunwald, J. E., Riva, C. E., Brucker, A. J., Sinclair, S. H. and Petrig, B. L., Altered retinal vascular response to 100% oxygen breathing in diabetes mellitus. *Ophthalmology*, 1984, **91**, 1447–1452.
13. Feke, G. T., Buzncy, S. M., Ogasawara, H., Fujio, N., Goger, D. G., Spack, N. P. and Gabbay, K. H., Retinal circulatory abnormalities in type 1 diabetes. *Investigations in Ophthalmology and Visual Science*, 1994, **35**, 2968–2975.
14. Deutsch, T. A., Read, J. S., Ernest, J. T. and Goldstick, T. K., Effects of oxygen and carbon dioxide on the retinal vasculature in humans. *Archives of Ophthalmology*, 1983, **101**, 1278–1280.
15. Riva, C. E., Grunwald, J. E. and Sinclair, S. H., Laser Doppler velocimetry study on the effect of pure oxygen breathing on retinal blood flow. *Investigations in Ophthalmology and Visual Science*, 1983, **24**, 47–51.
16. Hague, S., Hill, D. W. and Crabtree, A., The calibre changes of retinal vessels subject to prolonged hyperoxia. *Experimental Eye Research*, 1988, **47**, 87–96.
17. Dollery, C. T., Hill, D. W. and Hodge, J. V., The response of normal retinal blood vessels to angiotensin and noradrenaline. *Journal of Physiology*, 1963, **165**, 500–507.
18. Dollery, C. T., Hodge, J. V. and Engel, M., Studies of the retinal circulation with fluorescein. *British Medical Journal*, 1962, **2**, 1210–1215.